Australian Government
Department of Defence
Defence Science and
Technology Organisation

Assessment of Governor Control Parameter Settings of a Submarine Diesel Engine

Peter Hield and Michael Newman

Maritime Platforms Division
Defence Science and Technology Organisation

DSTO-RR-0386

ABSTRACT

Modern conventional submarines use diesel generators to provide power for propulsion and the hotel load. The governor, often a proportional-integral controller, attempts to maintain a constant speed by regulating the fuel flow to compensate for the back pressure disturbances due to the underwater exhaust. Poor control can cause fluctuating exhaust gas temperatures, leading to increased wear and reduced reliability. This paper develops a low order engine model which is then used to investigate the performance benefits that can be obtained through proper tuning of the governor control parameters. It is found that the engine exhibits stable behaviour over a very wide range of controller gains, and that tuning the governor solely to minimise the engine speed fluctuations may not minimise the exhaust gas temperature fluctuations.

Published by

Maritime Platforms Division
DSTO Defence Science and Technology Organisation
506 Lorimer St
Fishermans Bend, Victoria 3207 Australia

Telephone: (03) 9626 7000
Fax: (03) 9626 7999

AR-015-563
March 2013

APPROVED FOR PUBLIC RELEASE

Assessment of Governor Control Parameter Settings of a Submarine Diesel Engine

Executive Summary

Modern conventional submarines use diesel generators to provide power for propulsion and the hotel load. The governor, often a proportional-integral (PI) controller, attempts to maintain a constant speed by regulating the fuel flow to compensate for the back pressure disturbances due to the underwater exhaust. Poor control can cause fluctuating exhaust gas temperatures, leading to increased wear and reduced reliability.

This paper develops a low order model of a generic engine and governor, and then uses the model to examine the effect of varying the proportional and integral gains on the ability of the controller to reject the disturbance and maintain a constant engine speed. The effect of the governor gains on selected other engine parameters is also investigated.

The key conclusions from this work are as follows:

1. for a speed governed engine, with the control system implemented using a PI controller, the engine exhibits stable behaviour over very wide ranges of both the proportional and integral gains;
2. it is possible to tune the controller in such a way as to effectively eliminate engine speed fluctuations due to back pressure disturbances;
3. tuning the control system to focus on minimising speed fluctuations may, or may not, also minimise the cylinder exit temperature fluctuations (for the engine described in this paper, there is a large region for which the speed variations are minimised, but the cylinder exit temperature fluctuations are only minimised over a small part of this region); and
4. even at the optimal control point, a PI controller based on speed error alone still results in significant temperature variations due to exhaust back-pressure disturbances. This effect cannot be simply tuned out. A different control structure is required for reduced engine temperature variations.

It should be noted that the results presented in this paper only apply to the engine modelled here, and other engines may respond differently to changes in the controller gains. This paper describes a technique for optimising engine performance in response to back pressure fluctuations by tuning the controller parameters. In order to apply this technique to another engine, a validated model of that engine is required.

This page is intentionally blank

Authors

Peter Hield, Ph.D.
Maritime Platforms Division

Peter Hield received a Master of Engineering from Imperial College, London, in 2002. He completed a PhD at the University of Melbourne, titled "An experimental and theoretical investigation of thermoacoustic instability in a turbulent premixed laboratory combustor", graduating in 2008, and received the Dr John Patterson prize for the best thesis from the School of Engineering for this work.

He has previously worked in a variety of process industry Mechanical Engineering positions, before joining the Defence Science and Technology Organisation in February 2010. He currently works for the Propulsion and Energy Systems Group of Maritime Platforms Division, specialising in submarine diesel engines.

Michael Newman, Ph.D.
Maritime Platforms Division

Michael Newman completed his Bachelor of Science, Bachelor of Engineering (Electrical) and Doctor of Philosophy from Monash University, Australia, in 1997, 1999 and 2003, respectively.

Dr Newman's professional experience from 1996 until 2004 included employment with PowerCad Software, Adrian Newman & Assoc., and Creative Power Technologies. From 2004 until 2010 he worked in the USA for defence contractor General Atomics. His work focused on a variety of military and commercial projects, and included the design, manufacture, and qualification testing of power conversion systems for the US Navy in the 10s to 100s of Megawatts. As an engineering manager and senior engineer Dr. Newman, and the team he led, focused on projects such as the Electromagnetic Aircarft Launch System (EMALS) and Advanced Arresting Gear (AAG) programs for the US Aircraft Carrier fleet, as well as the Hybrid Electric Drive program for the US Navy DDG-51 class of ships. In 2010 he took on the role back in Australia as Head Propulsion & Energy Systems within the Maritime Platforms Division of DSTO.

This page is intentionally blank

Contents

This page is intentionally blank

Nomenclature

b	Empirical constant
c_p	Specific heat at constant pressure
c_v	Specific heat at constant volume
d	Diameter
e	Error
H	Enthalpy
I	Integral gain
J	Rotational inertia
k	Empirical constant
m	Mass flow rate
n	Number
N	Rotational speed
p	Pressure
P	Proportional gain
r	Ratio
R	Gas constant (air)
t	Time
T	Temperature
U	Internal energy
V	Volume
z	Discrete frequency domain transform variable

ε	Effectiveness
γ	Ratio of specific heats
η	Efficiency
μ	Isentropic temperature ratio
ρ	Density
τ	Torque

Subscripts and superscripts

c	Compressor, compression
cc	Combustion chamber
cmd	Commanded
comb	Combustion
corr	Corrected
cv	Control volume
cyl	Cylinder
d	Displaced
eng	Engine
f	Fuel
fr	Friction

in	Inlet
ind	Indicated
max	Maximum
min	Minimum
ND	Non-dimensional
out	Outlet
p	Pressure
pump	Pumping
ref	Reference
req	Required
res	Restriction
R	Crank revolutions per power stroke
vol	Volumetric
$\dot{g}$	Derivative with respect to time
g^*	Dimensionless

1. Introduction

Diesel generators typically operate at a constant engine speed and power a constant electrical load. One method of maintaining the desired engine operating point is to use a governor, which regulates the fuel flow rate in order to maintain a constant engine speed. A governor of this type is often all that is necessary for full control of the engine. For example, an increase in the load will cause a drop in engine speed, and, in response, the governor will increase the fuel flow rate until the speed is brought back to the set point. A common governor implementation is via a proportional-integral (PI) or proportional-integral-derivative (PID) controller. This paper only considers the simpler and more common PI-based control structure, with the impact of an added derivative component left for future work.

Under submarine snort conditions, the underwater exhaust system imposes a high exhaust back pressure on the diesel engine, due to a combination of the long exhaust ducting and the head of water above the exhaust outlet (see Figure 1). Sea surface waves passing over the submarine cause the water depth to vary, causing a corresponding fluctuation in the engine exhaust back pressure. This can result in fluctuations in the engine speed, air flow rate, fuel flow rate and cylinder temperature as the governor struggles to maintain constant speed [1-5]. Under high sea state conditions the engine power output must be reduced to limit the maximum cylinder temperatures, as excessive temperatures cause increased wear, reduced reliability and reduced engine life [1, 6].

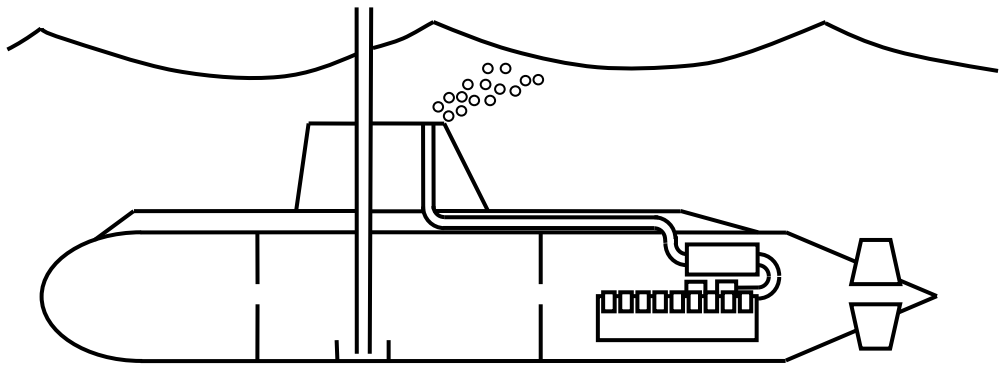

Figure 1 Diagram of a snorting submarine

Hield [1] developed a one dimensional computational fluid dynamic (CFD) model of a generic diesel in the submarine environment using the Ricardo Wave [7] engine modelling software (see Figure 2). The engine is an 11 litre six cylinder inline turbocharged diesel engine, similar in topology to those commonly used in conventional submarines. While useful for investigating engine behaviour, CFD models are non-linear and can be computationally intensive. From a control systems viewpoint, a submarine engine and governor form a standard closed loop control system, with the back pressure acting as a disturbance input to the system (see Figure 3). The dynamic behaviour of systems of this type is more easily examined using low order models. Such models are quick to run and can be linearised around an operating point, allowing the use of standard linear analysis techniques.

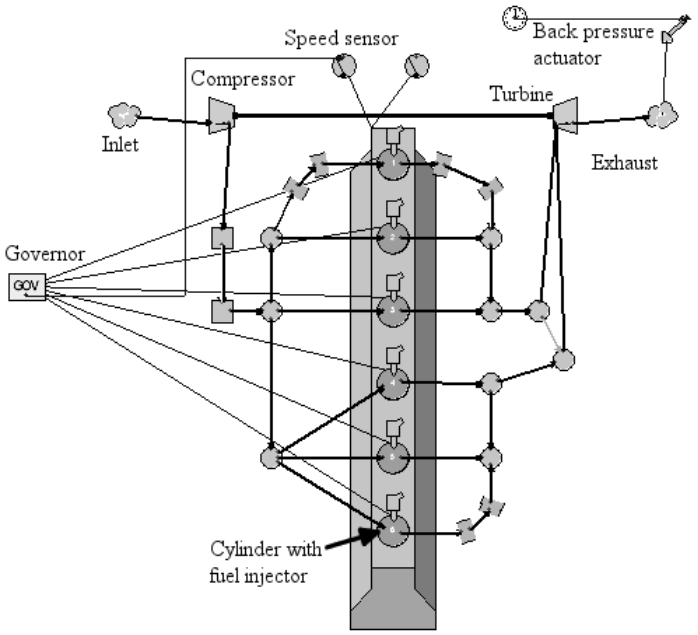

Figure 2 Ricardo Wave model of a speed-governed generic diesel engine in the submarine environment [1]

This paper develops a low order model of the engine and governor modelled by Hield [1], and then uses the model to examine the effect of varying the proportional and integral gains on the ability of the controller to reject the disturbance and maintain a constant engine speed. In this low order model, individual combustion events are not directly captured. Instead, the mean effect of the combustion is modelled and the time delays due to the intermittent nature of reciprocating engine combustion are captured in the engine control system model. In addition, the structure of the model allows any engine architecture to be modelled using different combinations of the engine component sub-models. The effect of the governor gains on selected other engine parameters is also investigated.

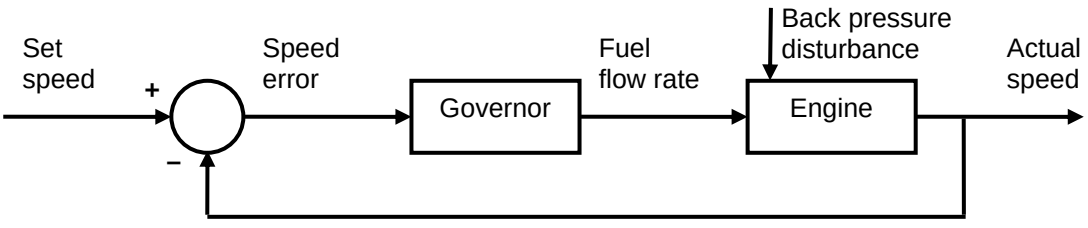

Figure 3 Diagram of the engine control system

2. The Model

There are many mean value engine models available in the literature (e.g. [8-13]). They all follow a similar structure, and model most engine components in the same way. There are, however, differences in the approaches taken, particularly with the modelling of the combustion chamber. The model described in this paper is an adaptation of that of Biteus [8], but takes sub-models from other authors where appropriate.

2.1 Model Structure

The gas path model consists of engine components separated by control volumes. Components define the mass flow based on the inlet and outlet conditions, and either add energy to or subtract energy from the flow. Components include compressors, turbines, combustion chambers, intercoolers and restrictions. Control volumes represent the manifolds connecting the engine components. The pressure and temperature of the gas within a control volume is set by the mass and enthalpy flows in and out of the control volume. By maintaining the order component – control volume – component, the flows can be balanced between the components and conflicts will not arise.

Non gas path models include rotating shafts and the engine governor and fuel system. Rotating shafts are used to transfer work between components and to the engine load. The governor monitors the engine speed and regulates the fuel flow rate in order to maintain the engine at the desired speed.

Using these models, it is possible to build low order engine models of a wide variety of engine architectures, including naturally aspirated, supercharged, turbocharged engines, or combinations of these.

2.1.1 The Compressor Model

Supercharged and turbocharged engines use a compressor to increase the pressure of the intake air, increasing the mass of air that can be inducted into the cylinders and therefore increasing the power that can be obtained from the engine. Compressor characteristics cannot be calculated from first principles. Instead they are measured experimentally and presented in the form of maps relating the compressor speed and efficiency to the mass flow and pressure ratio.

The mass flow through the compressor and the isentropic efficiency are obtained from

$$\dot{m}_c = f_1\left(r_{pc}, N_c\right), \tag{1}$$

and

$$\eta_c = f_2\left(r_{pc}, N_c\right), \tag{2}$$

where

$$r_{pc} = \frac{p_{out}}{p_{in}}. \tag{3}$$

Refer back to the nomenclature section at the beginning of the paper for the meaning of the symbols. The temperature of the gas leaving the compressor is obtained from the definition of the isentropic efficiency

$$T_{out} = T_{in}\left(1+\frac{1}{\eta_c}\left(\mu_c - 1\right)\right), \tag{4}$$

and the compressor torque is given by

$$\tau_c = \frac{\dot{m}_c c_p T_{in}}{\eta_c N_c}\left(\mu_c - 1\right), \tag{5}$$

where μ_c is the compressor isentropic temperature ratio

$$\mu_c = r_{pc}^{(\gamma-1)/\gamma}. \tag{6}$$

Equations (1) and (2) are the compressor maps, and, as defined here, relate the mass flow and efficiency to the pressure ratio and speed. The mass flow and speed data can, however, be presented in one of several different forms, and appropriate conversions must be made depending on the form of the available data.

2.1.2 The Turbine Model

On a turbocharged engine, the compressor is powered by a turbine, which extracts energy from the exhaust gases. The mass flow through the turbine and the isentropic efficiency are obtained from

$$\dot{m}_t = f_3\left(r_{pt}, N_t\right), \tag{7}$$

and

$$\eta_t = f_4\left(r_{pt}, N_t\right), \tag{8}$$

where

$$r_{pt} = \frac{p_{in}}{p_{out}}. \tag{9}$$

Note that the definition of the pressure ratio is the opposite to that for the compressor. These definitions are adopted by convention, in order to obtain number greater than unity in both cases. The temperature of the gas leaving the turbine is obtained from the definition of the isentropic efficiency

$$T_{out} = T_{in}\left(1-\eta_t\left(1-\frac{1}{\mu_t}\right)\right), \tag{10}$$

and the turbine torque is given by

$$\tau_t = \frac{\dot{m}_t c_p T_{in} \mu_t}{N_t}\left(1-\mu_t\right), \tag{11}$$

where μ_t is the turbine isentropic temperature ratio

$$\mu_t = r_{pt}^{(\gamma-1)/\gamma}. \tag{12}$$

Equations (7) and (8) are the turbine maps, and, as defined here, relate the mass flow and efficiency to the pressure ratio and speed. As for the compressor, the mass flow and speed

data can be presented in a number of forms and appropriate conversions are required before using the map data.

2.1.3 The Combustion Chamber Model

The combustion chamber is the most important part of the diesel engine. It is the component where energy is added to the system and also the component which applies a torque to the crankshaft in order to drive the load. Diesel engines can operate on either the two- or four-stroke cycles. In either case, air is inducted into the cylinder and compressed. Fuel is injected and burnt, increasing the pressure and temperature of the gas in the cylinder, which then applies a torque to the crankshaft via the pressure on the piston. The exhaust gases are then expelled from the cylinder and replaced with fresh air.

This is an inherently discrete process, but can be modelled as a continuous process by calculating only the mean values of the combustion chamber parameters. A diesel engine approaches this ideal as the number of cylinders increases.

The mass flow through the combustion chamber is given by

$$\dot{m}_{cc} = \frac{1}{2\pi} \frac{\rho_{in} V_d n_{cyl} N_{eng} \eta_{vol}}{n_R}, \tag{13}$$

where the factor of 2π converts the rotational speed of the engine from radians per second to revolutions per second, and the density is calculated from the ideal gas equation of state

$$\rho_{in} = \frac{p_{in}}{R T_{in}}. \tag{14}$$

The volumetric efficiency is given by

$$\eta_{vol} = \frac{r_c}{r_c - 1} - \frac{1}{\gamma (r_c - 1)} \left(\frac{p_{out}}{p_{in}} + \gamma - 1 \right). \tag{15}$$

The exit temperature is obtained from an energy balance as

$$T_{out} = T_{in} + \frac{\eta_{comb} LCV_f \dot{m}_f}{\dot{m}_{cc} c_v}. \tag{16}$$

The torque is difficult to obtain correctly from first principles as is depends on a large number of factors. As the aim of this model is to examine submarine diesel engines, correct modelling of the effect of back pressure is important. Although automotive diesels experience some back pressure from the exhaust pipe and in particular from exhaust after-treatment equipment such as catalytic converters, the levels are much lower than those experienced by submarine engines, and the back pressure does not vary in the same way. Some mean value engine models do not account for back pressure in the calculation of the torque (e.g. [10, 11, 14]), but others (e.g. [9, 12]) do include it, and Hopka *et al*. [9] describes the effect of the back pressure as "highly influential". Even when the back pressure is included, there is no agreement as to how this should be done. For example Wahlström and Eriksson [12] model the 'pumping torque' (the torque required to pump the air through the cylinder against the resistance due to the back pressure), as

$$\tau_{pump} = \frac{V_d}{4\pi}\left(p_{out} - p_{in}\right). \tag{17}$$

This pumping torque is subtracted from the indicated torque and so appears as a loss in the system. Hopka *et al*. [9] obtain the 'indicated torque' from an empirical relationship

$$\tau_{ind} = b_1\dot{m}_f + b_2\frac{\dot{m}_f}{N_{eng}} + b_3\dot{m}_{cc} + b_4 N_{eng}\left(p_{out} - p_{in}\right) + b_5 T_{in}, \tag{18}$$

which includes the pumping losses (note the slightly different definition of indicated torque), and this is the approach adopted here. The empirical constants can be obtained by a least squares regression fit to data from either experimental testing or Ricardo Wave simulations of the engine to be modelled.

2.1.4 Restriction and Heat Exchanger Models

Elements such as filters, exhaust after-treatment, butterfly valves and heat exchangers can result in a mass flow rate dependent pressure drop as the air flows through them, and are modelled as restrictions in the flow. In addition, energy can be removed from the flow either incidentally via heat losses from pipes or deliberately through an intercooler or an exhaust gas cooler for exhaust gas recirculation systems. This is modelled using the heat exchanger equations.

An intercooler, which reduces the temperature of the flow but also results in a pressure drop, can be modelled as a single component by combining a restriction with a heat exchanger in the same component.

The mass flow through a restriction is calculated assuming a quadratic relationship between mass flow and pressure drop

$$\dot{m}_{res} = \sqrt{\frac{\rho_{in}\left(p_{in} - p_{out}\right)}{k_{res}}}, \tag{19}$$

where the density is again obtained from the ideal gas equation of state. The exit temperature of the flow through a heat exchanger is calculated using

$$T_{out} = T_{in} - \varepsilon\left(T_{in} - T_{amb}\right), \tag{20}$$

where the heat exchanger effectiveness may be either a constant or an empirical function of the air mass flow. If there is no heat loss (e.g. in the case of a filter), the exit temperature is set equal to the inlet temperature.

2.1.5 The Control Volume Model

Control volumes represent the ducting between the separate engine components. They have a finite volume and can therefore store mass and energy. The quantity of stored mass and energy can be calculated based on the flows into and out of the control volume. The pressure and temperature of the gas within the control volume can then be calculated from the stored mass and energy.

The mass stored within the control volume is calculated from the mass conservation equation

$$m_{cv} = \int \dot{m}_{in} - \dot{m}_{out} dt, \tag{21}$$

and the energy stored from the first law of thermodynamics

$$U_{cv} = \int \dot{H}_{in} - \dot{H}_{out} dt, \tag{22}$$

where the enthalpy flow into the control volume is found from the temperature and mass flow rate of the inlet air flow

$$\dot{H}_{in} = \dot{m}_{in} c_p T_{in}. \tag{23}$$

The pressure within the control volume is obtained from the equation of state

$$p_{cv} = \frac{R U_{cv}}{V_{cv} c_v}, \tag{24}$$

and the temperature from the ideal gas energy-temperature relationship

$$T_{cv} = \frac{U_{cv}}{m_{cv} c_v}. \tag{25}$$

The enthalpy flow out of the control volume can then be obtained from

$$\dot{H}_{out} = \dot{m}_{out} c_p T_{cv}. \tag{26}$$

2.1.6 The Shaft Model

Within an engine, shafts transfer mechanical energy between components. They are typically the crankshaft, which connects the combustion chamber(s) to the load and may also drive a compressor (in the case of a supercharged engine) and the turbocharger shaft, which, for a turbocharged engine, connects the turbine to the compressor.

A shaft is modelled using Newton's second law for rotating components. Friction may be modelled either as a torque

$$\tau_{in} - \tau_{out} - \tau_{fr} = J \frac{dN}{dt}, \tag{27}$$

or as a loss from the system

$$k_{fr} \tau_{in} - \tau_{out} = J \frac{dN}{dt}. \tag{28}$$

2.1.7 The Engine Control and Fuel System Models

In a general sense, engine control systems may take as inputs a wide variety of parameters, including engine speed, load, ambient pressure, ambient temperature engine temperature, boost pressure, exhaust emissions concentrations and many others. These parameters are then used by the control system to keep the engine operating within set limits, which may include speed, output power, acceleration, emissions limits as well as many other factors. The most basic form of engine control for diesel engines is the speed governor, and this is the system modelled here. The aim of this control system is to maintain a constant engine speed, and it does so by regulating the mass flow rate of the fuel. This system is particularly useful for power generation or marine propulsion diesel engines. A similar method can also be used to model other forms of engine control system.

The engine control system is modelled as a standard feedback control loop, with a PI controller. The speed error is given by

$$e = N_{eng,setpoint} - N_{eng,actual} \tag{29}$$

and the required fuel mass flow is then given by

$$\dot{m}_{f,req} = Pe + I\int e dt. \tag{30}$$

The fuel delivery system has a finite response time which is primarily due to the discrete nature of reciprocating engines, in which a small quantity of fuel is injected in a short burst at a specific point in the engine cycle. Regardless of the demand from the controller, the fuel system cannot respond until the next cylinder reaches this point in its cycle. In addition to this, there are finite limits on the quantity of fuel that can be delivered.

The fuel system is modelled as a saturation to provide upper and lower limits on the fuel mass flow rate

$$\dot{m}_{f,cmd} = \begin{cases} \dot{m}_{f,max} & if \quad \dot{m}_{f,max} \le \dot{m}_{f,req} \\ \dot{m}_{f,req} & if \quad \dot{m}_{f,min} < \dot{m}_{f,req} < \dot{m}_{f,max} \\ \dot{m}_{f,min} & if \quad \dot{m}_{f,req} \le \dot{m}_{f,min} \end{cases} \tag{31}$$

and the effect of the discrete injection events is modelled as an integer delay, with the delay period given by the time between successive cylinders firing

$$\dot{m}_f = z^{-1}\dot{m}_{f,cmd}. \tag{32}$$

Simulink allows the use of both continuous and discrete sub-models within the same model, so that the most accurate model can be obtained for each component. For the model stability calculations discussed in Section 4.1, the model was linearised at its operating point using the Simulink Control Design Toolbox. For this linearisation, the Tustin method was used to approximate the discrete delay as a continuous system

$$z = \frac{1 + sT/2}{1 - sT/2}. \tag{33}$$

2.2 Turbocharged Diesel Engine Model

The components described above were used to create a low order engine model of the 11L inline 6 cylinder turbocharged diesel engine modelled by Hield [1]. The gas path of the engine model consists of a compressor, intercooler, combustion chamber and turbine, separated by three control volumes representing the inlet and exhaust manifolds. There are two shafts, representing the crankshaft and the turbocharger shaft, a control system and a fuel system. A schematic of the model layout is shown in Figure 4.

The information required for the low order engine model was taken from the Ricardo Wave model, including the engine geometry and turbocharger maps. The Ricardo Wave model was run over a wide range of operating conditions, and the resulting data used to obtain the empirical constants required by the combustion model.

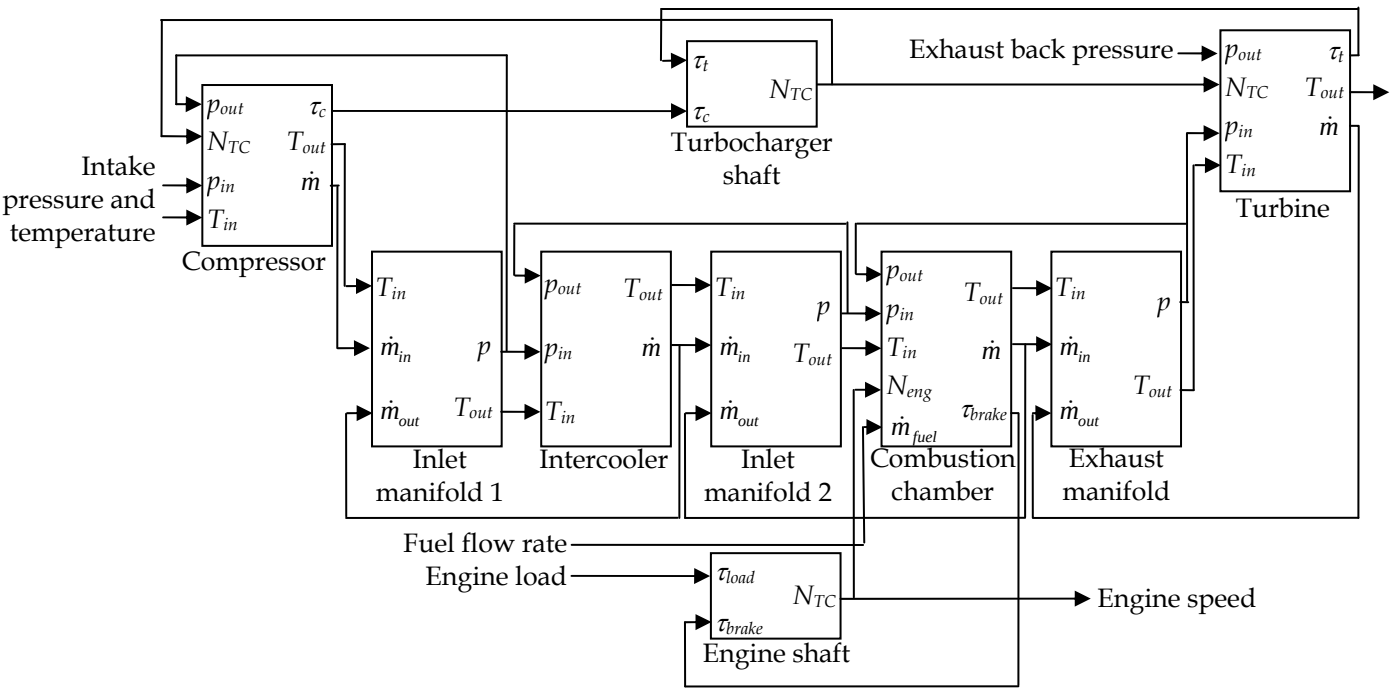

Figure 4 The turbocharged diesel engine model

3. Validation of the Model

The model was validated against results from the Ricardo Wave model described by Hield [1]. Each component was validated individually by providing the component with the inputs seen by the equivalent component in the Ricardo Wave model, and comparing the component outputs against those from the Ricardo Wave model. Figure 5 shows the outputs of the compressor model for both the Ricardo Wave model and the low order model. The compressor exit temperature predicted by the low order model closely matches that predicted by the Ricardo Wave model. However the mass flow rate predicted by the low order model is slightly low, due to small differences in the compressor maps used in each case. This then causes a slight under prediction of the torque required to drive the compressor. However the trends in response to the disturbance are captured well by the low order model. Although not shown here, similar results were obtained for all the other components in the low order model.

Five whole-engine simulations were used for model validation: a step increase in load; a step increase in speed; a step increase in back pressure; back pressure variations representative of sea state 3; and back pressure variations representative of sea state 6. The results are shown in Figure 6 to Figure 10.

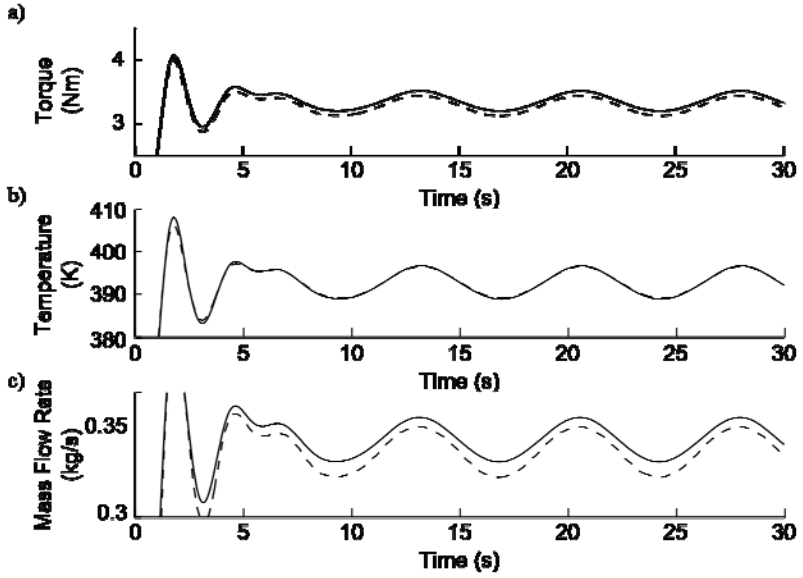

Figure 5 Ricardo Wave (———) and low order (– – –) model results for the compressor validation under sea state 3 back pressure conditions. a) The torque required to drive the compressor, b) the compressor exit temperature and c) the mass flow rate through the compressor.

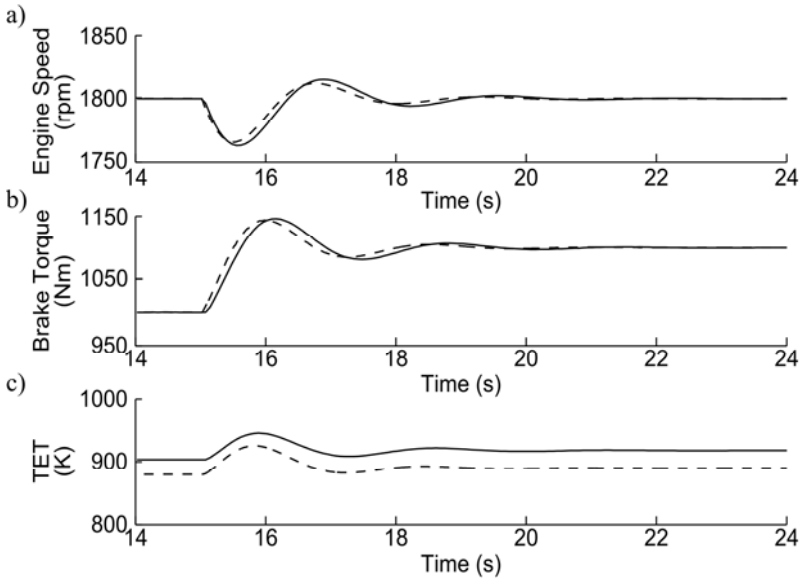

Figure 6 Ricardo Wave (———) and low order (– – –) model results for a step increase in load. a) The engine speed, b) the brake torque and c) the turbine entry temperature.

The validation shows that the low order engine model is capable of replicating the behaviour of the more detailed Ricardo Wave engine model very well. In particular, the engine speed and brake torque are accurately predicted for steady state conditions. The predicted turbine entry temperature is too low for most operating conditions, although the trend is captured accurately. Figure 6 to Figure 8 show that the response of the brake torque to changes in operating condition is too quick in the low order engine model, although once again the trend is captured. These errors are due to the combustion chamber model, which does not fully capture all the effects of varying the back pressure, and requires further work. Figure 9 shows

that the engine response to sea state 3 conditions is very well predicted by the low order engine model, although the model accuracy decreases as the sea state increases with some higher frequency components appearing in the torque and speed results (see Figure 10). One interesting feature is that both the Ricardo Wave model and the low order engine model predict small amplitude high frequency fluctuations in the torque response, probably due to the governor responding too quickly to the relatively slowly varying engine operating conditions.

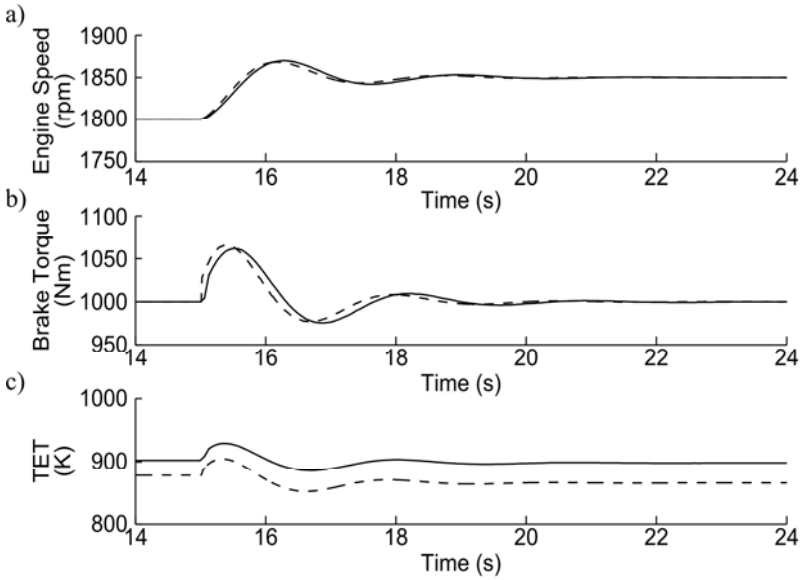

Figure 7 Ricardo Wave (———) and low order (– – –) model results for a step increase in engine speed. a) The engine speed, b) the brake torque and c) the turbine entry temperature.

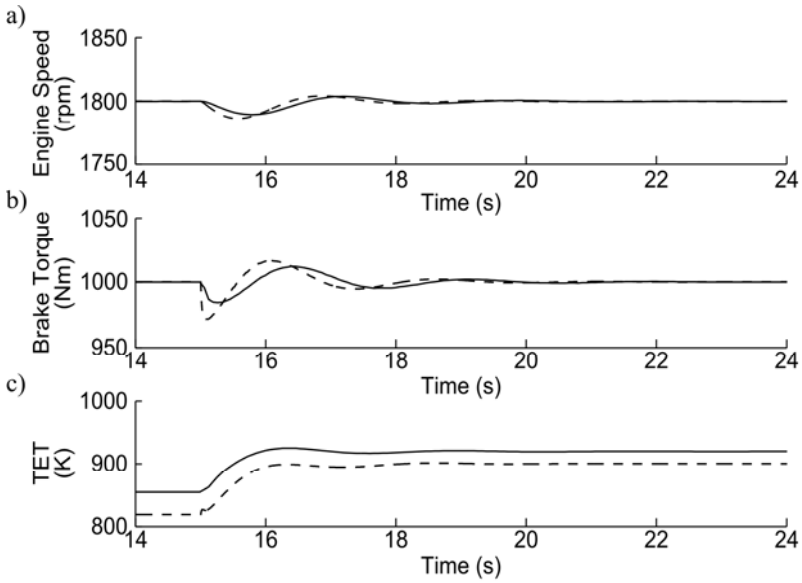

Figure 8 Ricardo Wave (———) and low order (– – –) model results for a step increase in back pressure. a) The engine speed, b) the brake torque and c) the turbine entry temperature.

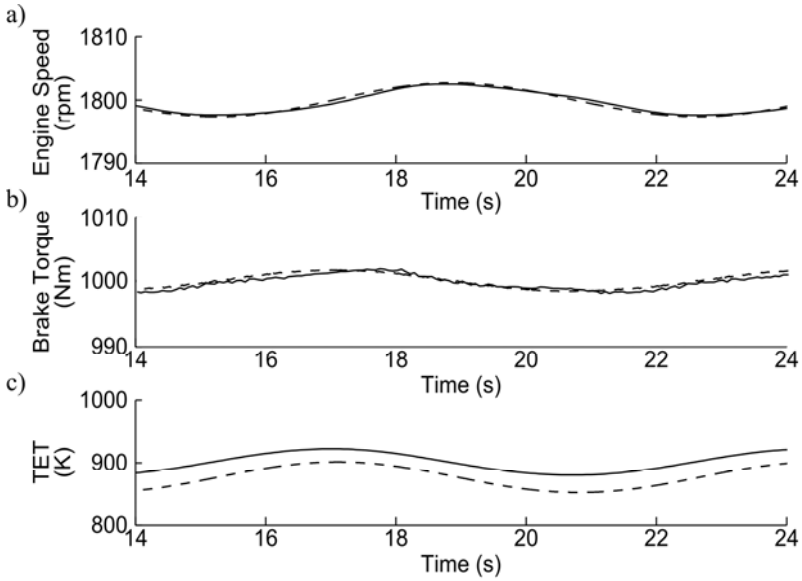

Figure 9 Ricardo Wave (———) and low order (– – –) model results for sea state 3 back pressure conditions. a) The engine speed, b) the brake torque and c) the turbine entry temperature.

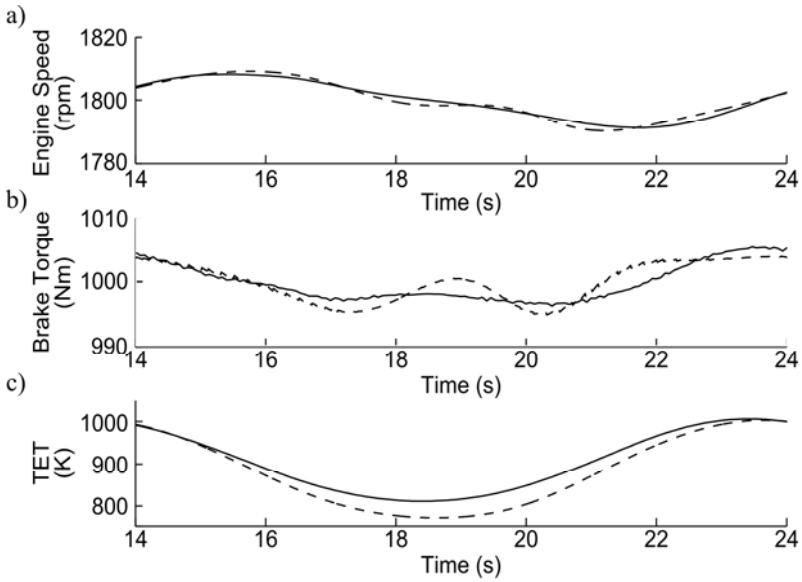

Figure 10 Ricardo Wave (———) and low order (– – –) model results for sea state 6 back pressure conditions. a) The engine speed, b) the brake torque and c) the turbine entry temperature.

Although not shown here, it was found that the low order engine model results were extremely sensitive to small changes in the turbocharger maps used as inputs to the model (see Sections 2.1.1 and 2.1.2). Turbocharger maps cannot be determined theoretically and must be measured. The data therefore contains a small amount of scatter, and a polynomial surface must be fitted through the data in order for it to be used in a Simulink model, which requires evenly spaced data points on a rectangular grid. There is a large number of possible data fits,

depending on the order of the polynomials used, and the choice of polynomial can significantly affect the results of the low order engine model. Thus care must be taken when choosing the data fit for the turbocharger maps.

4. The Effect of the Governor Gain Settings

The low order engine model was used to investigate the effect of varying the engine governor gains on the ability of the control system to reject imposed back pressure disturbances. The model was run for a wide range of values of P and I, and the system performance was evaluated at each point. Several measures of system stability and performance were calculated, and the results are discussed in this section.

4.1 System Stability

Two common measures of relative stability of a linear system are the phase and gain margins. The phase margin is defined as 180° plus the phase angle of the open loop transfer function at the gain crossover frequency (the frequency at which the gain is unity). The gain margin is the reciprocal of the gain of the open loop transfer function at the frequency where the transfer function phase angle is -180° [15, 16]. For stable engine operation, both the phase margin and the gain margin (expressed in dB) must be positive.

The low-order diesel engine model contains several non-linear terms and so needed to be linearised before the phase and gain margins could be calculated. This was done using Simulink's Control Design toolbox. Although the linear approximation to the model would vary significantly over the whole operating range of the engine, this paper is concerned with the operation of the engine as a generator. Thus the engine is only operated at a single operating point. The applied sinusoidal back pressure disturbance causes the engine operating point to move away from that for the steady state, however it has been confirmed that this does not significantly change the linear approximation to the model. In each case, the simulation time at which the model was linearised was chosen such that the calculated stability was conservative.

Figure 11 shows the variation of the system phase margin as a function of P and I, with the variation in gain margin over the same range shown in Figure 12. The model predicts stable engine operation over a very wide range of both P and I, which may be varied by several orders of magnitude (note the logarithmic scales used for the P and I axes).

When both P and I were set to low values it was not possible to run the model. This is because the controller gains are too low for the system to respond to disturbances sufficiently quickly to keep the engine operating parameters within an acceptable range. A step change in the engine load, for example, would cause the engine to stall as the engine speed would drop too far before the fuel flow increased to compensate for the increased load. This region has been marked as having insufficient gain. For low I but larger values of P, the model predicts stable operation up to a threshold of $P \approx 0.2$ above which the phase margin rapidly decreases and unstable behaviour is predicted. Within this band of P values, I can be reduced to zero

without affecting the stability of the system. For low P but larger values of I, stable behaviour is predicted, which gradually becomes unstable as I is increased further. The value of I at which instability sets in increases as P increases. At the centre of Figure 11 is a large region representing the values of the controller gains P and I for which the model predicts that the engine will respond to back pressure disturbances in a stable manner.

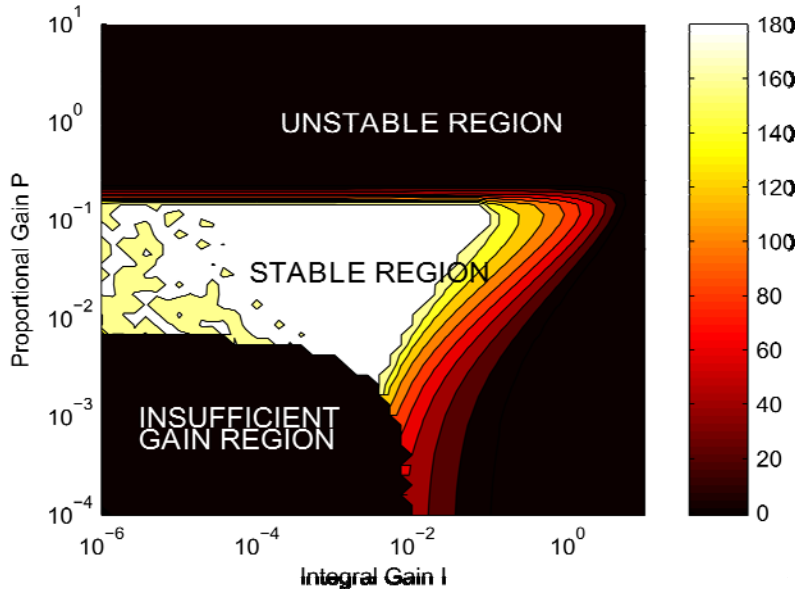

Figure 11 The system phase margin stability indicator as a function of P and I

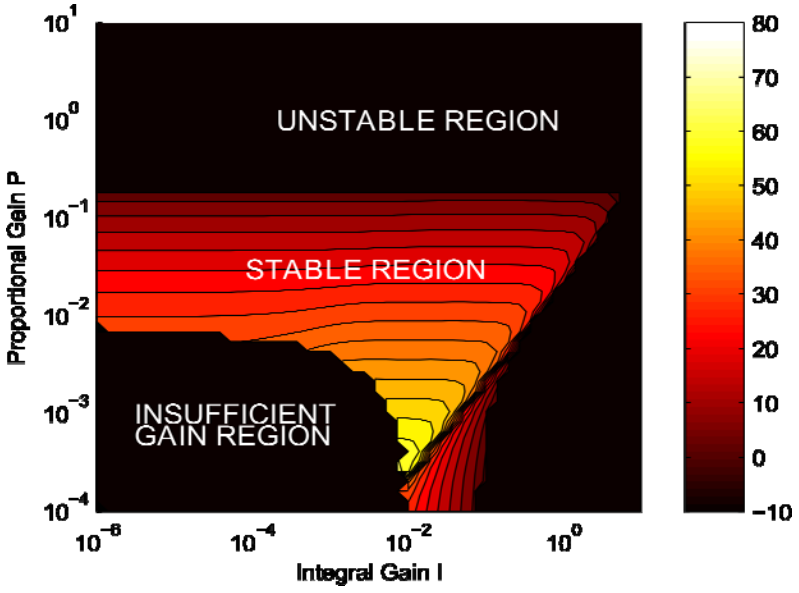

Figure 12 The system gain margin stability indicator as a function of P and I

The threshold P value appears to be independent of the value of I. The unstable behaviour in the region is due to the delays inherent in the fuel system. For a six cylinder 4-stroke engine operating at 1800 rpm, one cylinder fires every $1/90^{th}$ of a second. Thus, even if the controller detects an error in the engine speed, the fuel system is incapable of responding until the next cylinder fires, thus introducing a delay of up to $1/90^{th}$ of a second. The speed error may grow during this time, and a large proportional gain will produce a large corrective action when the cylinder does fire, potentially leading to an overcorrection and thus unstable behaviour. The threshold I value is due to the delay introduced by the integration of the error signal. The significance of this delay increases as I increases relative to P, and thus P cannot be reduced to zero for any value of I.

The theoretical stability point of the linearised system is independent of the sea state conditions, as the varying exhaust back-pressure is treated as a disturbance into the system and not a change to the closed loop control system structure. Therefore, the results above are presented independent of the sea state condition. However, while the system may be stable for a given operating point, for large disturbances on the system (such as varying exhaust back pressure under high sea state conditions) the response of the engine parameter may still be undesirable (or even unacceptable). Under excessive disturbance conditions the validity of the linearised system may also be affected. For these reasons the transient response of the system to disturbances as the PI control gains are varied also need to be investigated.

4.2 Sea State 3 Disturbance Response

Sea state 3 conditions were represented by a sine wave back pressure disturbance superimposed on the mean back pressure. The amplitude was 6.25 kPa (corresponding to a significant wave height of 1.25 m) and a period of 7.4 s. The peak-peak speed variation for sea state 3 conditions is shown in Figure 13. Contours are plotted over the stable region of the P-I space. As the task of the engine governor is to maintain a constant speed, the amplitude of the speed variation provides the primary measure of the controller performance. This is close to zero over most of the stable region, although there is a ridge of severe speed fluctuations along the line of $P \approx 10I$. The amplitude of the speed fluctuations reduces gradually as P and I are moved away from this line, in some areas requiring a variation of P or I by up to two orders of magnitude before the amplitude is reduced to zero.

A second performance metric is the peak-peak variation of the cylinder exit temperature (see Figure 14). This follows a similar pattern to the engine speed fluctuations, although adjusting I has progressively less effect to the left of the line $P \approx 10I$. Also, the peak-peak variation of the cylinder exit temperature remains significant over the whole range of stable values of P and I. Thus, with a speed governor as the sole means of controlling an engine subject to fluctuations in the back pressure, it is possible to reduce but not completely eliminate the cylinder exit temperature fluctuations.

The maximum cylinder exit temperature is shown in Figure 15. This performance metric follows a pattern significantly different from the fluctuations in engine speed and cylinder exit temperature, and can be split into two distinct regions. To the left of the line $P \approx 10I$, the maximum cylinder exit temperature is independent of I, but strongly dependent on P, decreasing with increasing P. To the right of this line, the maximum cylinder exit temperature

is approximately constant at its minimum value, and is independent of both P and I. There is only a small region close to the line $P \approx 10I$ where the value of I has a significant effect.

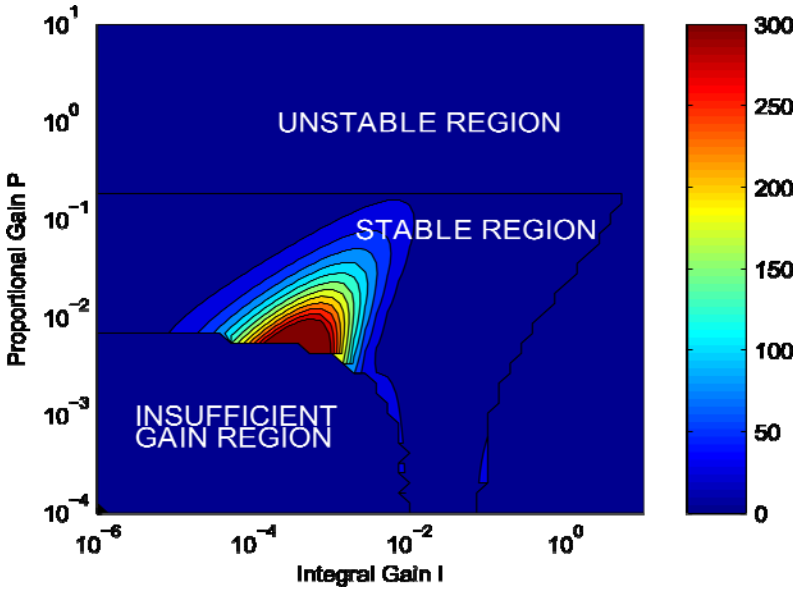

Figure 13 The peak-peak variation in shaft speed (rpm) as a function of P and I, for sea state 3 conditions

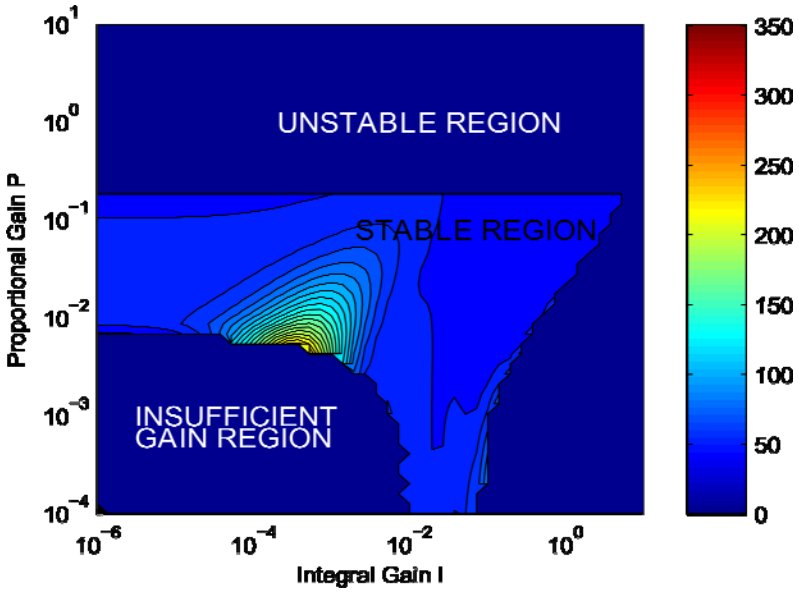

Figure 14 The peak-peak variation in the cylinder exit temperature (K) as a function of P and I, for sea state 3 conditions

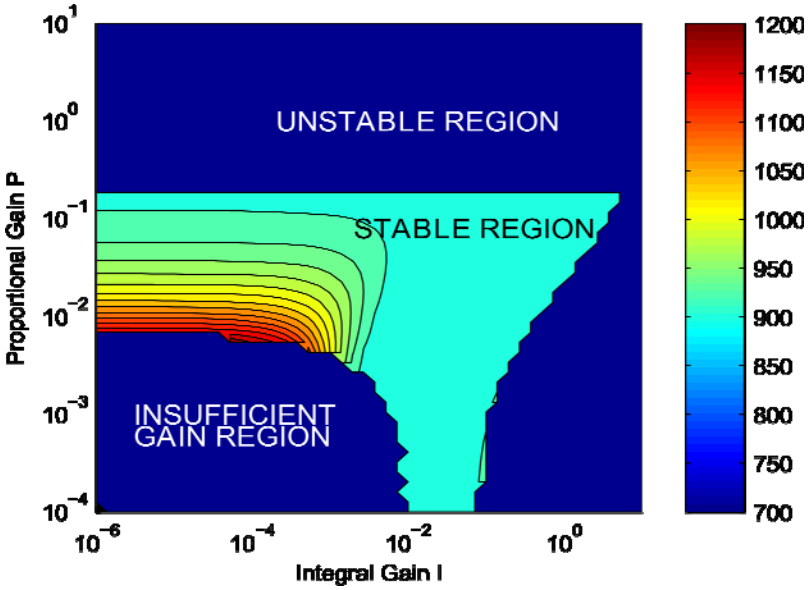

Figure 15 The maximum cylinder exit temperature (K) as a function of P and I, for sea state 3 conditions

Other performance measures are also possible, and, although not shown here, the peak-peak variation in the turbocharger shaft speed was also considered. This showed very similar behaviour to the peak-peak variation in the engine speed, although the minimum value was significant, at ~20,000 rpm peak-peak. This is due to the pressure ratio across the turbine being directly affected by the back pressure disturbance, and not directly controlled by the engine speed governor.

The stability and performance parameters can be used to impose further limits on the range of acceptable values of *P* and *I*. This allows trade offs to be examined and the optimal values selected when tuning the controller gains. Although a system is stable for positive phase and gain margins, it is usual to allow a safety factor to keep the operating point well away from the stability boundaries and to compensate for modelling errors. In this case, a phase margin of 45° and a gain margin of 20 dB have been selected. Regions for which the phase and gain margins are below these values are highlighted in Figure 16, in light green and light blue, respectively.

Similar boundaries can also be placed on the performance measures. The region for which the maximum temperature is more than 20 K above the optimal operating point has been highlighted in red on Figure 16 as a region to avoid when tuning the controller. Similarly, the region for which the peak-peak speed variation exceeds 25 rpm is highlighted in green, and the region in which the peak-peak temperature variation is more than 20 K higher than the optimal operating point is highlighted in orange. This leaves the area highlighted in dark blue as the preferred region for setting the *P* and *I* control gains. This is quite a large area, covering almost two orders of magnitude for *I* and three orders of magnitude for *P*. Figure 13 to Figure 15 show the controller performance improves as both *P* and *I* are increased, although for sufficiently high values of *P* and *I*, further increases have only a minimal effect. Figure 11 and

Figure 16 show that the limiting factor on the maximum values of P and I is the system stability.

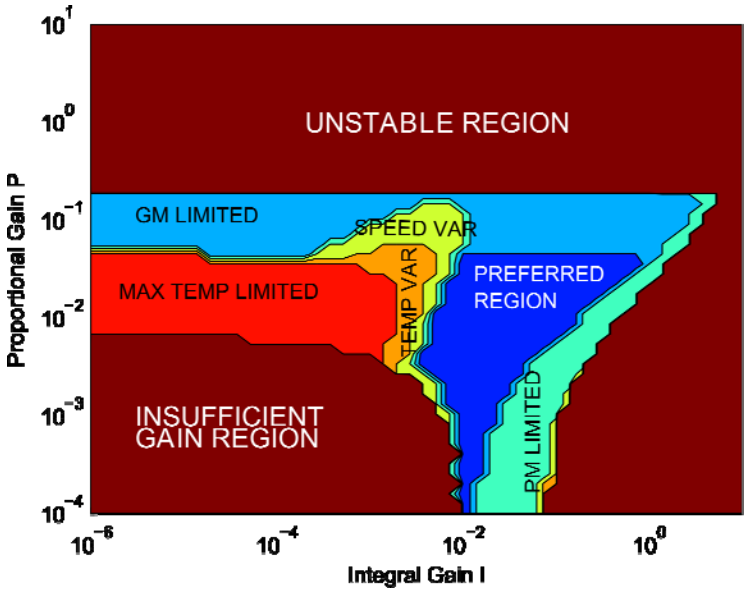

Figure 16 The limiting stability and performance metrics over the region of allowable values of P and I, for sea state 3 conditions. Colours indicate the limiting parameter which makes operation undesirable at certain values of P and I. Preferred region (■), gain margin limited (■), phase margin limited (■), maximum temperature limited (■), amplitude of temperature fluctuations limited (■) and amplitude of speed variations limited (■).

4.3 Sea State 6 Disturbance Response

Sea state 6 was investigated using the same approach as applied in the previous section for sea state 3. The amplitude of the back pressure disturbance was 30 kPa (corresponding to a significant wave height of 6 m) and a period of 10.3 s. The results are shown in Figure 17 to Figure 20. Comparison of Figure 17 with Figure 13 shows that the increase in sea state has only a marginal effect on the shaft speed variation, increasing the range of values of P and I over which low amplitude shaft speed variations occur, but not affecting the values of P and I for which the maximum shaft speed variations occur, or the amplitude of those variations. However, comparison of Figure 18 and Figure 19 with Figure 14 and Figure 15 shows that the increase in sea state results in an increase in both the exhaust temperature variation and the maximum exhaust temperature. In particular, while the maximum temperature increases almost uniformly over the whole range of P and I values, the amplitude of the temperature variation does not. Figure 18 shows the increase in sea state resulted in an increase in the temperature variations for low values of I that was much larger than that for high values of I. This shows clearly that tuning the governor gains for a single sea state based on the engine shaft speed variation alone may not produce optimum performance overall.

The resulting preferred region (blue) for selection of control parameters shown in Figure 20 is clearly smaller than that presented in Figure 16. As previously discussed, there is no change in the stability region as this limit is independent from the disturbance. However, the change in

engine response due to the increase in the amplitude of the applied disturbance results in a more constrained preferred operating region.

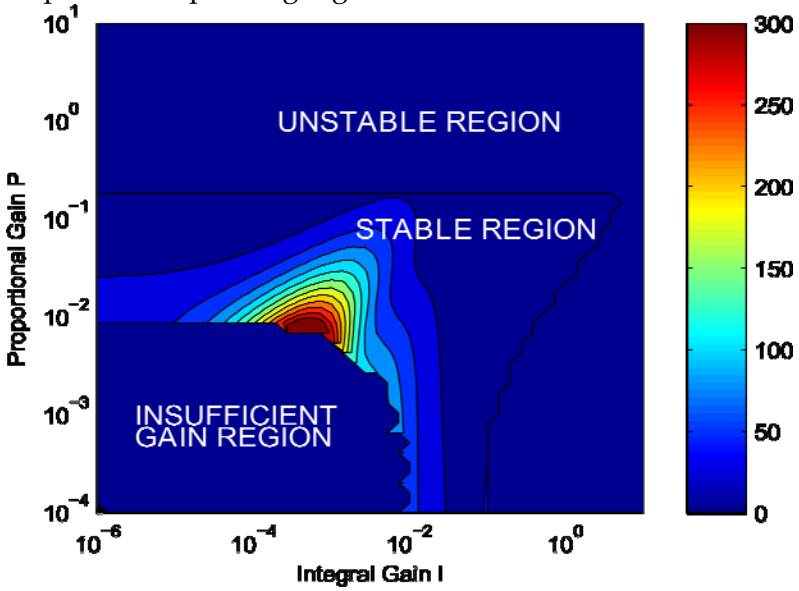

Figure 17 The peak-peak variation in shaft speed (rpm) as a function of P and I, for sea state 6 conditions

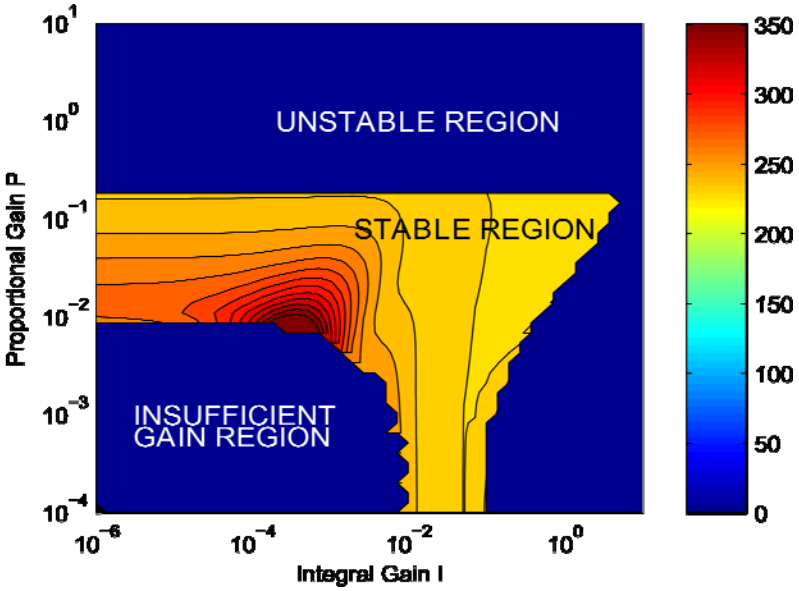

Figure 18 The peak-peak variation in the cylinder exit temperature (K) as a function of P and I, for sea state 6 conditions

While occurrences of snorting in sea state 6 conditions is not likely to be common, it is still a plausible condition that the submarine will have to be able to support. For simplicity of design, implementation and operation it is not desirable to have different control gains for different operating conditions. Luckily, in this case the preferred region for the higher sea state condition is simply a sub-set of the lower sea state condition. Therefore, by selecting

control gains within the preferred region of the worse case sea state, the conditions for all required sea states can be met.

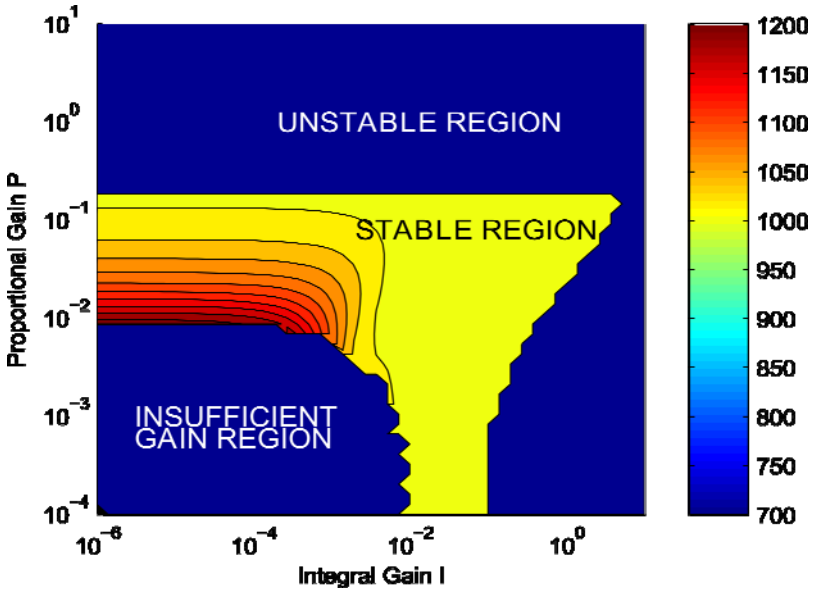

Figure 19 The maximum cylinder exit temperature (K) as a function of P and I, for sea state 6 conditions

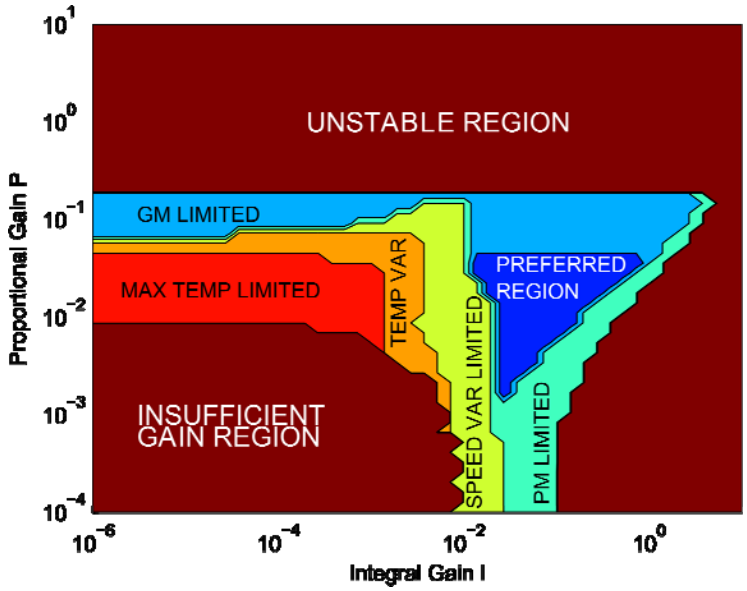

Figure 20 The limiting stability and performance metrics over the region of allowable values of P and I, for sea state 6 conditions. Colours indicate the limiting parameter which makes operation undesirable at certain values of P and I. Preferred region (), gain margin limited (), phase margin limited (), maximum temperature limited (), amplitude of temperature fluctuations limited () and amplitude of speed variations limited ().

5. Conclusion

Matlab/Simulink has been used to create a low order model of a diesel engine, which was then validated against a more detailed Ricardo Wave engine model. The engine control system consists of a speed governor which monitors the engine speed and varies the fuel flow with the aim of matching the engine speed to the set speed. The speed governor was implemented using a PI controller. An exhaust back pressure disturbance was applied to simulate the engine operating conditions for a snorting submarine. The model structure allows any engine architecture to be modelled simply by rearranging the sub-models representing the engine components.

The model was used to examine the engine behaviour for different values of the controller gains P and I, with a back pressure disturbance representative of sea state 3. Stable engine behaviour was predicted over a very wide range of values of both P and I, and both can be adjusted by several orders of magnitude while still allowing the engine to operate successfully. However, there were significant variations in engine performance over this range and with a poor choice of the controller gains, large fluctuations in the engine speed, turbocharger shaft speed and cylinder exit temperature will occur, along with excessively high maximum cylinder exit temperatures. The results show that a good choice of P and I can reduce the engine speed fluctuations effectively to zero, and significantly reduce the maximum cylinder exit temperature. For the engine modelled in this paper, this is achieved by increasing both gains as much as possible, while being mindful that increasing the gains too far will lead to instability. Optimising the controller gains to minimise the engine speed fluctuations also minimises the cylinder exit temperature fluctuations, the turbocharger shaft speed variations and the maximum cylinder exit temperature.

The control system examined here only targets engine speed. Although it is possible to eliminate the fluctuations in engine speed with this control strategy, it is not possible to eliminate the fluctuations in cylinder exit temperature. In addition, the value of a performance metric which is insignificant for particular values of P and I at one sea state may be significant at another. Thus it is important to tune the engine based on all important performance metrics, and to do so for all sea states for which the engine is expected to perform satisfactorily.

The key conclusions from this work are therefore as follows:

1. for a speed governed engine, with the control system implemented using a PI controller, the engine exhibits stable behaviour over very wide ranges of both the proportional and integral gains;
2. it is possible to tune the controller in such a way as to effectively eliminate engine speed fluctuations due to back pressure disturbances;
3. tuning the control system to focus on minimising speed fluctuations may, or may not, also minimise the cylinder exit temperature fluctuations (for the engine described in this paper, there is a large region for which the speed variations are minimised, but the cylinder exit temperature fluctuations are only minimised over a small part of this region); and

4. even at the optimal control point, a PI controller based on speed error alone still results in significant temperature variations due to exhaust back-pressure disturbances. This effect cannot be simply tuned out. A different control structure is required for reduced engine temperature variations.

It should be noted that the results presented in this paper only apply to the engine modelled here, and other engines may respond differently to changes in the controller gains. This paper describes a technique for optimising engine performance in response to back pressure fluctuations by tuning the controller parameters. In order to apply this technique to another engine, a validated model of that engine is required.

6. References

1. Hield, P. A. (2011) *The effect of back pressure on the operation of a diesel engine*. DSTO-TR-2531, [Technical Report] Melbourne, Vic., Defence Science and Technology Organisation (Australia)
2. van den Pol, E. (1990) Aspects of submarines, part IV: The submarine and the diesel engine. *SenW 57STE* (JAARGANG NR 5)
3. Goodwin, G., McGrath, J. and Bowden, D. (2008) Performance of turbocharged diesel engines in ocean-going submarines. In: *Pacific 2008, International Maritime Conference,* Sydney, IMarEST
4. Kirkman, E. T. F. and Hopper, R. A. (1990) Turbocharging for submarines - A special case. In: *International Conference on Turbochargers and Turbocharging*, IMechE
5. Mann, J. (2011) Twin-turbocharged diesel performance under snorkelling conditions. In: *UDT 2011,* London
6. Challen, B. and Baranescu, R. (1999) *Diesel engine reference book*. 2nd ed. Bath, Butterworth-Heinemann
7. Ricardo (2010) *Wave 8.2 Help System*
8. Biteus, J. (2004) *Mean value engine model of a heavy duty diesel engine*. LITH-ISY-R-2666, [Technical Report] Linkoping, Sweden, Department of Electrical Engineering, Linkopings Universitet
9. Hopka, M., Upadhyay, D., Guezennec, Y. and Rizzoni, G. (2003) Identification of a mean value model of a modern diesel engine for control design. In: *2003 ASME International Mechanical Engineering Congress,* Washington, D. C.
10. Vasu, J., Deb, A. K., Mukhopadhyay, S. and Pattada, K. (2011) Development and validation of an MVEM from an SI-engine based WCCM. In: *Proceedings of 2011 International Conference on Modelling, Identification and Control,* Shanghai, China
11. Wang, H., Tang, H. and Sun, J. (2012) Modeling and simulation of marine diesel propulsion system in ship maneuvering condition. *Advanced Materials Research* **354-355** 472-477
12. Wahlström, J. and Eriksson, L. (2006) *Modeling of a diesel engine with VGT and EGR including oxygen mass fraction*. LiTH-ISY-R-2747, [Technical Report] Linkoping, Sweden, Department of Electrical Engineeing, Linkopings Universitet
13. Eriksson, L. (2007) Modeling and Control of Turbocharged SI and DI engines. *Oil and Gas Science and Technology* **62** (4) 523-538

14. Karmiggelt, R. (1998) *Mean value modelling of a s.i. engine*. Report Number 98.041, Eindhoven, Eindhoven University of Technology
15. Ogata, K. (1997) *Modern control engineering*. Upper Saddle River, NJ, Prentice-Hall
16. DiStephano, J., Stubberud, A. and Williams, I. (1976) *Theory and problems of feedback and control systems*. Los Angeles, CA, McGraw Hill

DEFENCE SCIENCE AND TECHNOLOGY ORGANISATION
DOCUMENT CONTROL DATA

1. PRIVACY MARKING/CAVEAT (OF DOCUMENT)

2. TITLE

Assessment of Governor Control Parameter Settings of a Submarine Diesel Engine

3. SECURITY CLASSIFICATION (FOR UNCLASSIFIED REPORTS THAT ARE LIMITED RELEASE USE (L) NEXT TO DOCUMENT CLASSIFICATION)

Document	(U)
Title	(U)
Abstract	(U)

4. AUTHOR(S)

Peter Hield and Michael Newman

5. CORPORATE AUTHOR

DSTO Defence Science and Technology Organisation
506 Lorimer St
Fishermans Bend Victoria 3207 Australia

6a. DSTO NUMBER	6b. AR NUMBER	6c. TYPE OF REPORT	7. DOCUMENT DATE
DSTO-RR-0386	AR-015-563	Research Report	March 2013

8. FILE NUMBER	9. TASK NUMBER	10. TASK SPONSOR	11. NO. OF PAGES	12. NO. OF REFERENCES
2011/1138525/1	07/360	DGSMC	25	16

13. DSTO Publications Repository

http://dspace.dsto.defence.gov.au/dspace/

14. RELEASE AUTHORITY

Chief, Maritime Platforms Division

15. SECONDARY RELEASE STATEMENT OF THIS DOCUMENT

Approved for public release

OVERSEAS ENQUIRIES OUTSIDE STATED LIMITATIONS SHOULD BE REFERRED THROUGH DOCUMENT EXCHANGE, PO BOX 1500, EDINBURGH, SA 5111

16. DELIBERATE ANNOUNCEMENT

No Limitations

17. CITATION IN OTHER DOCUMENTS Yes

18. DSTO RESEARCH LIBRARY THESAURUS

Diesel Engines, Submarine Engines, Propulsion Systems, Control

19. ABSTRACT

Modern conventional submarines use diesel generators to provide power for propulsion and the hotel load. The governor, often a proportional-integral controller, attempts to maintain a constant speed by regulating the fuel flow to compensate for the back pressure disturbances due to the underwater exhaust. Poor control can cause fluctuating exhaust gas temperatures, leading to increased wear and reduced reliability. This paper develops a low order engine model which is then used to investigate the performance benefits that can be obtained through proper tuning of the governor control parameters. It is found that the engine exhibits stable behaviour over a very wide range of controller gains, and that tuning the governor solely to minimise the engine speed fluctuations may not minimise the exhaust gas temperature fluctuations.